Supporting Information

Hierarchical Porous Covalent organic framework/graphene composite aerogel for High-Performance Supercapacitors

Ning An, Zhen Guo, Jiao Xin, Yuanyuan He, Kefeng Xie, Daming Sun, Xiuyan Dong, Zhongai Hu*

*Corresponding author. E-mail: anning@mail.lzjtu.cn (N. An)

S1 Experimental Section

S1.1 Analysis and characterization

The morphologies of products were observed by using a field-emission scanning electron microscope (FESEM; ULTRA plus, Germany). UV-Vis-NIR spectra were recorded in transmission geometry using a UV-3600 Plus spectrometer equipped with a 150 mm InGaAs integrating sphere. The absolute fluorescence quantum yields were measured on HITACHI F-7100 by using an integrating sphere. The crystallinity of the samples was tested on X-ray diffraction (D/Max-2400, Japan) at the Cu Kα radiation (λ=0.15418 nm) in the 2θ range of 0°-70°. The chemical structures of the samples were recorded on a Fourier transform infrared spectra (FT-IR, VERTEX 70, Germany Bruker) with KBr pellets in the wavelength range of 4000-400 cm^{-1}. Zeta potential was measured using a Malvern Zetasizer Nano ZS ZEN 3600 (Malvern Instruments, USA). Nitrogen adsorption–desorption isotherms were measured on a Micromeritics ASAP 2020 gas adsorption analyzer at 77 K. The Brunauer-Emmett-Teller (BET) method was utilized to calculate the specific surface areas and pore volume, the NLDFT method was applied for the estimation of pore size distribution.

S1.2 Materials

Sulfuric acid (98%, H_2SO_4), Cetyltrimethylammonium bromide (96%, CTAB), 2, 6 Diaminoanthraquinone (97%, DAAQ) were obtained from Alfa Aesar Chemicals Co. Ltd., Shanghai, China. 1,3,5-triformylphloroglucinol (Tp) and 1,3,5-Trimethylbenzene

was purchased from Aladdin Industrial Corporation. *N, N*-Dimethylformamide (DMF) and dioxane was purchased from Tianjin Damao Chemical Reagent (Tianjin, China). All the experiments were carried out using deionized (DI) water and analytical reagents. GO was prepared from pure graphite powder by a modification of the Hummers method.[1, 2]

S1.3 Sample preparation

S1.3.1 Synthesis of DAAQ-COFs Materials

1,3,5-triformylphloroglucinol (Tp, 10 mg, 0.048 mmol) was mixed with 2,6-diaminoanthraquinone (DAAQ, 17 mg, 0.071 mmol) in a mortar-pestle. After the mixture was uniformly grinded for 3 minutes, few drops of 3 M Ac(OH) (~5-10 μL) was added. Continue to grind the mixture until the powder turns orange. Collect the above orange solids and put them into the glass pressure tube (18 cm of length, 25 mL). Add the mesitylene/dioxane = 1/1 (v/v) solution (3 mL) and of 3 M Ac(OH) (0.6 mL) to the pressure tube. The tube was sealed off and then heated at 120 °C for 72 h. The red precipitate was collected by filtration and rinsed with N,N-dimethylformylamide (DMF), tetrahydrofuran (THF) and ethanol in turn. The powders were collected and dried at 60 °C for 24 h.

S1.3.2 Synthesis of DAAQ-COFs/GA Materials

The DAAQ-COFs/GA nanocomposite was prepared by the electrostatic self-assembly combined with hydrothermal method. Firstly, the prepared DAAQ-COFs (5-15 mg) were added into 5 mL NaOH aqueous solution (pH=10.0) and dispersed by ultrasonic for 5 min. Then add CTAB (1.5 mg) and stir for 20 min until it is completely dissolved.

GO (30 mg) was ultrasonicated in 10 mL of distilled water for 30 min to obtain a homogeneous brown solution. Then, a specified concentration of positively charged CTAB-COFs dispersion with DAAQ-COFs/GO weight ratios from 1/6 to 1/2 was added into the negatively charged GO dispersion and stirred for 2 h at room temperature. After the electrostatic self-assembly is completed, the suspension was poured into a Teflon-lined autoclave and heated at 180 °C for 12 h. The prepared gel nanocomposite remained floating in the solution, and the color of the solution becomes clear. After being cooled naturally to ambient temperature, the as-prepared DAAQ-COFs/GA was rinsed extensively with distilled water to remove any impurities. Finally, the obtained DAAQ-COFs/GA was freeze-dried under vacuum.

S1.3.3 Synthesis of GA Materials

The 3D GA was prepared by hydrothermal reduction of GO aqueous dispersion. 30 mL homogeneous GO solution (2.0 mg mL^{-1}) sealed in a 50 mL Teflon-lined autoclave maintained at 180 °C for 12h. After the autoclave was naturally cooled down to room temperature, the prepared gel was repeatedly washed with DI water and 3D graphene monolith was obtained by freeze-drying.

S1.4 Electrochemical Characterizations

In three-electrode system, the glassy carbon electrode (d=5 mm) was used as current collector, the working electrode was prepared as follow: 4 mg of as-prepared sample and 0.7 mg acetylene black were dispersed in 0.4 mL of 0.25 wt% Nafion after milling sufficiently. Then 6 μL above suspension was dropped onto the current collector by using of the pipet gun, and then dried under room temperature. The carbon rod and saturated calomel electrode were used as counter electrode and reference electrode, respectively, and the 1.0 M H_2SO_4 was used as electrolyte. A series of electrochemical

measuring techniques including cyclic voltammogram (CV) and galvanostatic charge-discharge (CD), which were performed on a CHI 660E electrochemical workstation (Shanghai CH Instruments, China). Electrochemical impedance spectroscopy (EIS) was measured by a Autolab electrochemical workstation (AUT87571, Switzerland). EIS was conducted in the frequency range of 10^5 -10^{-2} Hz with an amplitude of 5 mV. Cycling stability was measured by using a CT4008T Land battery tester (Wuhan Landian Electronic Co., China).

S1.5 Fabrication of Supercapacitors

The asymmetric supercapacitor was constructed using conventional coin-type device (CR 2032). The DAAQ-COF/GA and pure graphene aerogel was pressed and directly served as the working electrodes with area mass loading of ~3.5 mg cm^{-2}. The both electrodes in supercapacitor system was separated with a cellulose filter paper (Whatman®) and few ml of an aqueous acidic electrolyte (1 M H_2SO_4) was used as an electrolyte. The asymmetric supercapacitor was assembled by sandwiching an electrolyte separator between positive electrode (GA) and negative electrode (DAAQ-COF/GA) which mass ratio was calculated based on charge balanced formula (1)

$$Q = C \times V \times m \quad (1)$$

where C (F g^{-1}), V (V) and m (g) are specific capacitance, operating potential window and the mass of the active materials, respectively. The mass loading on both positive and negative electrodes was over 1 mg cm^{-2}.

S1.6 Calculations

(1) In three-electrode system, we calculated the capacitances of the supercapacitors based on both the CV curves and the GCD profiles. The integrated area under a CV curve is equivalent to the charge that is stored during the anodic scan and delivered during the cathodic scan. The specific capacitance can be calculated, according to the following equation:

$$C = \frac{\int id(V)dV}{mv\Delta V} \quad (2)$$

where $\int i(V)dV$ (V.s) is the integration of the current-potential curve during the

discharge, m (g) indicates the mass of the material loaded onto the electrode, ΔV (V) is the working voltage window, and ν (V s^{-1}) is the scan rate.

Specific capacitances also derived from galvanostatic tests can be calculated from the equation:

$$C = I\Delta t / mV \quad (3)$$

where m (g) is the mass of active electrode material in the working electrode, V (V) is the potential drop during discharge, Δt (s) is the discharge time and I (A) is the discharging current.

(2) In two-electrode system, specific capacitances of capacitor derived from galvanostatic tests can be calculated from the equation:

$$C = I\Delta t / mV \quad (4)$$

where m (g) is the total mass of active electrode material in two electrodes, V (V) is the voltage drop upon discharging, Δt (s) is the discharge time and I (A) is the discharging current.

Energy density (E) and power density (P) derived from galvanostatic tests can be calculated from the following equations:

$$E = [C (\Delta V)^2]/2 \quad (5)$$

$$P = E / \Delta t \quad (6)$$

where E (Wh kg^{-1}), P (W kg^{-1}), Δt (s), ΔV (s) and C (F g^{-1}) are the energy density, power density, discharge time, potential window, specific capacitance, respectively.

S2 Supplementary Figures and Tables

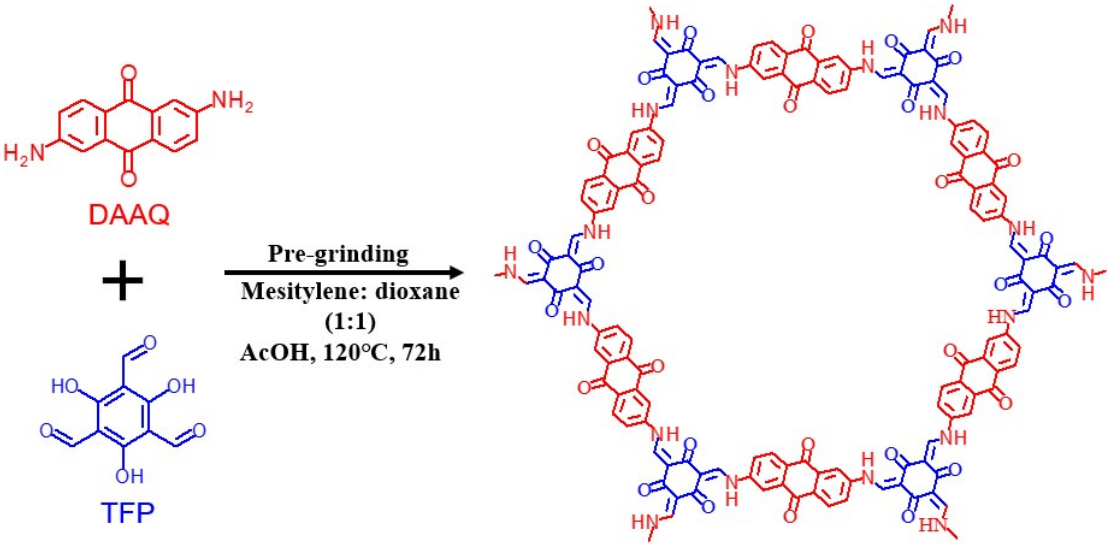

Figure S1. Synthesis of DAAQ-COFs.

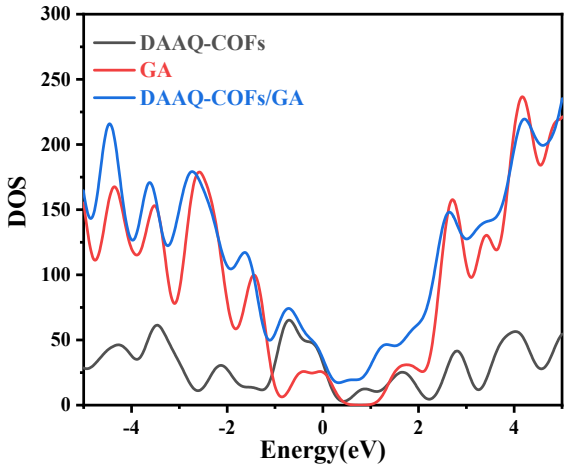

Figure S2. TDOS of pristine graphene, DAAQ-COFs and DAAQ-COFs/GA.

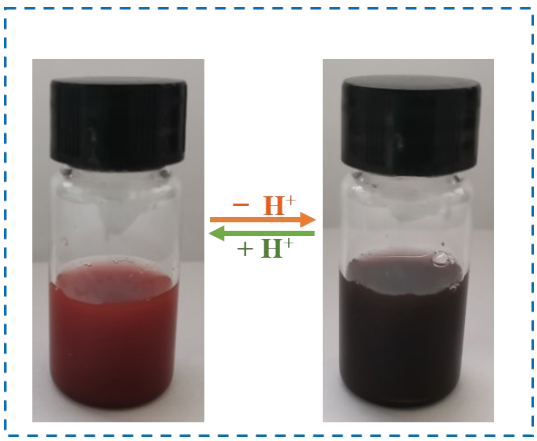

Figure S3. Digital photographs of DAAQ-COFs dispersion under neutral condition (pH = 7.0) (left) and alkaline condition (pH = 13.0) (right).

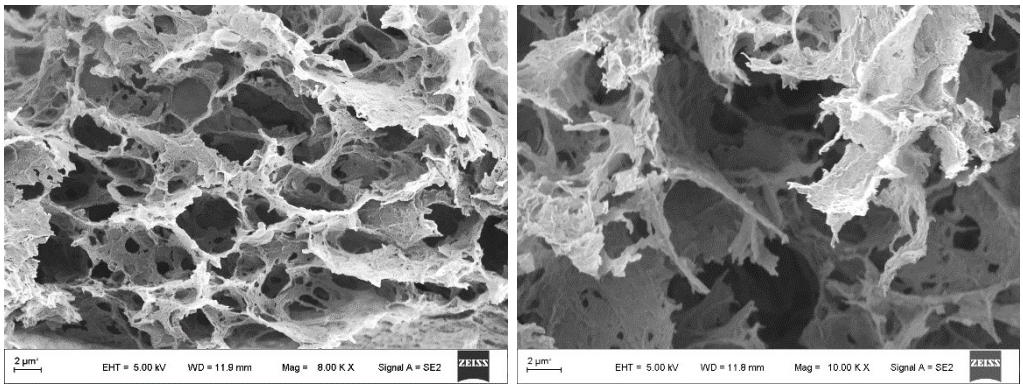

Figure S4. The SEM images of GA.

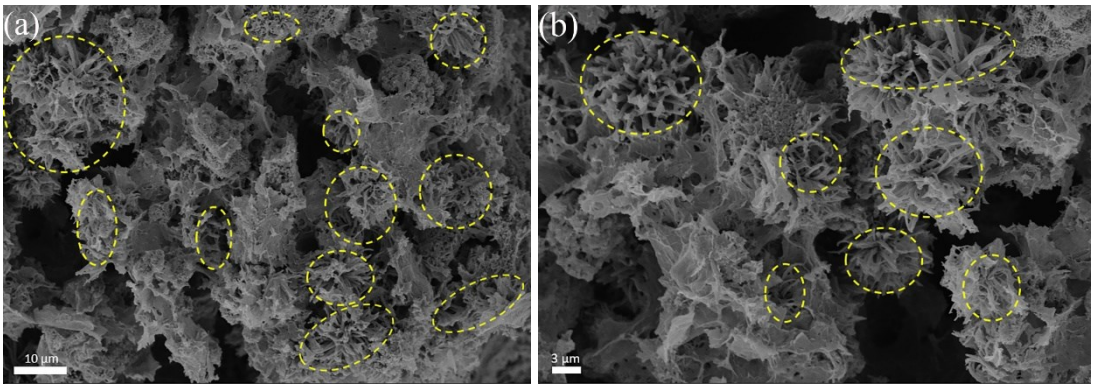

Figure S5. The SEM images of DAAQ-COFs (COF/GO=1/4) at different magnifications.

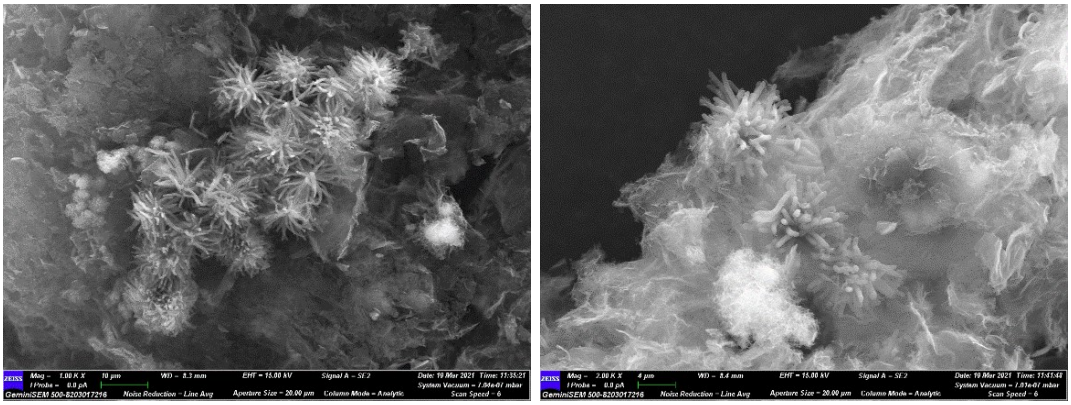

Figure S6. The SEM images of DAAQ-COFs/GA(COF/GO=1/2).

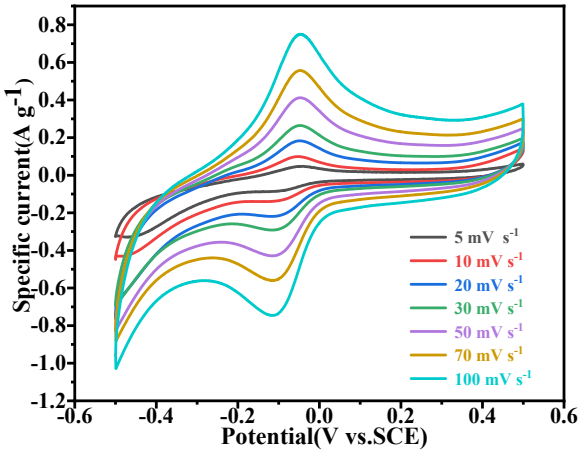

Figure S7. CV curves of an DAAQ-COFs electrode at different scan rates in 1.0 M H_2SO_4 solution. (5 to 100 mV s^{-1}).

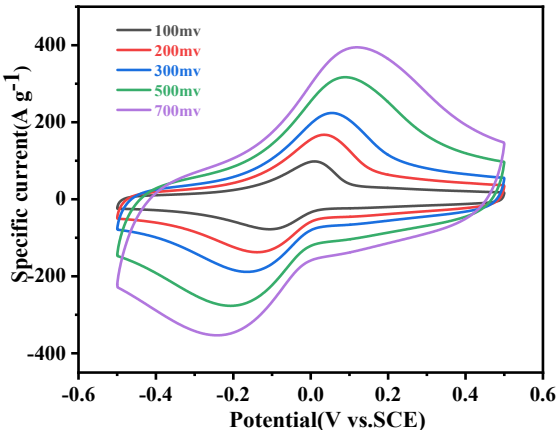

Figure S8. CV curves of an DAAQ-COFs/GA electrode at different scan rates in 1.0 M H_2SO_4 solution. (100 to 700 mV s^{-1}).

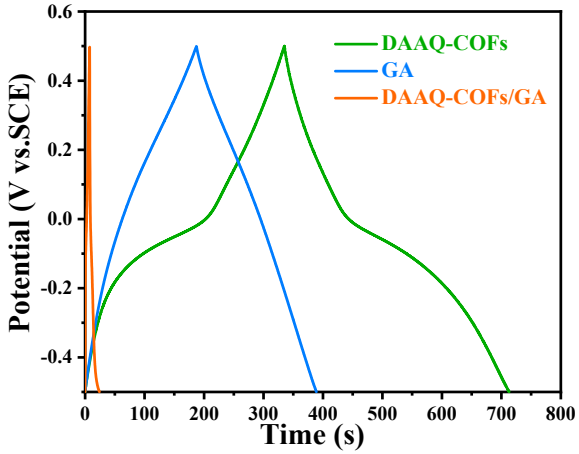

Figure S9. GCD curves of GA, DAAQ-COFs and DAAQ-COFs/GA at 1 A g^{-1}.

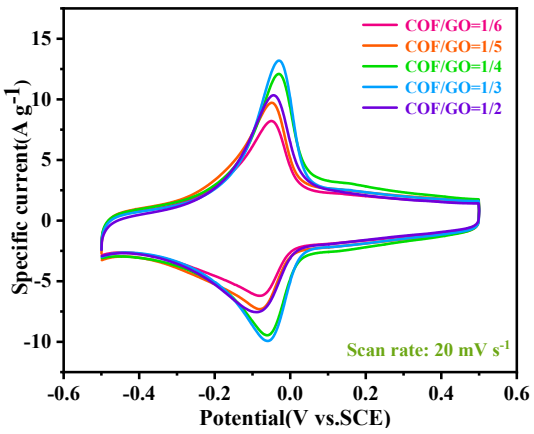

Figure S10. CVs of the DAAQ-COFs/GA electrode (at 20 mV s^{-1}) with different DAAQ-COFs: GO wt% ratios from 1/6 to 1/2.

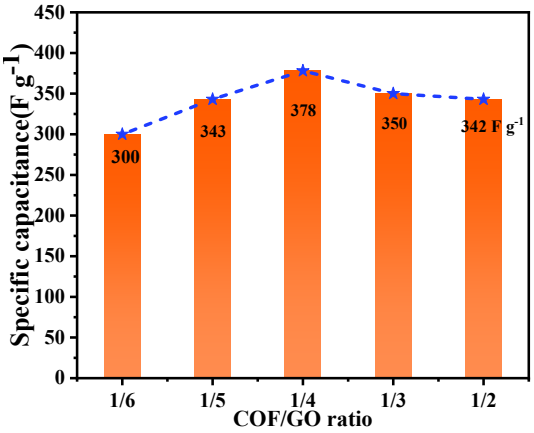

Figure S11. The specific capacitances of the as-synthesized DAAQ-COFs/GA electrodes with different ratios.

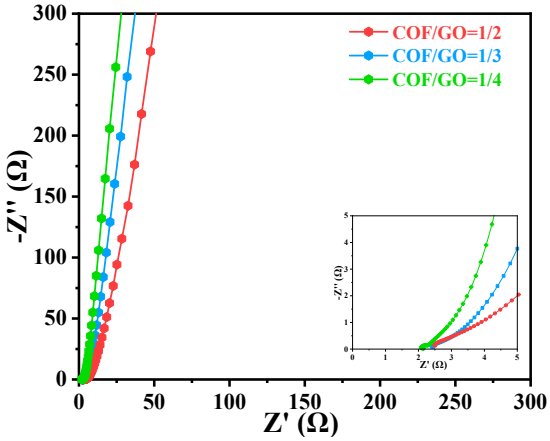

Figure S12. Nyquist plot of the DAAQ-COFs/GA electrodes.

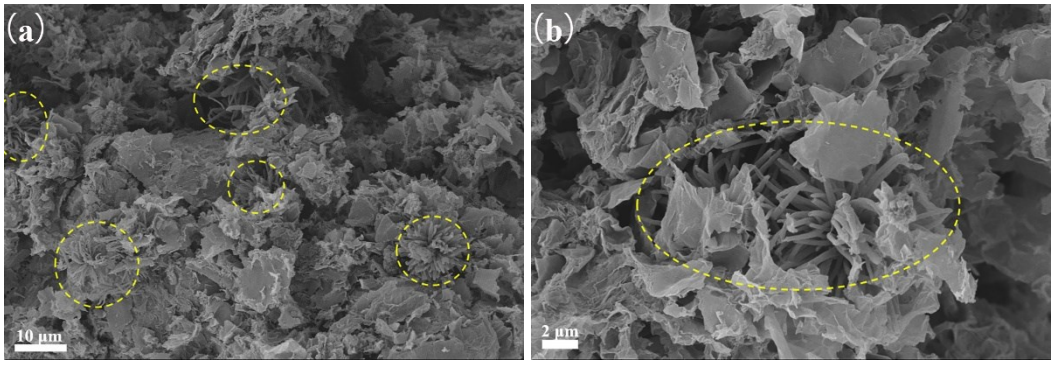

Figure S13. The SEM images of DAAQ-COFs/GA after cycling.

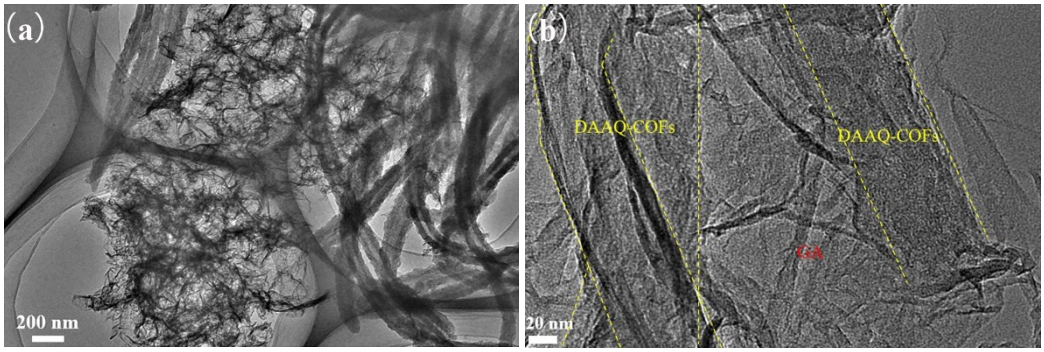

Figure S14. The TEM images of DAAQ-COFs/GA after cycling.

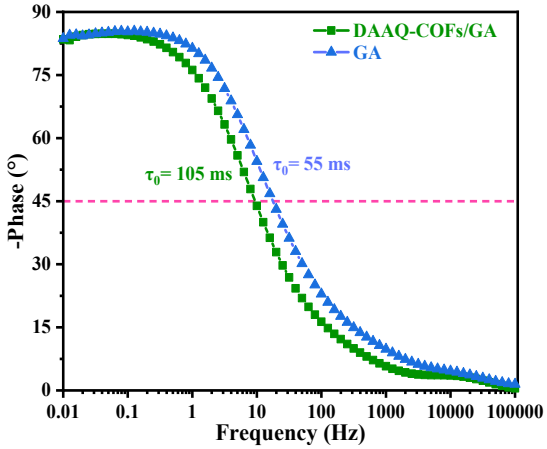

Figure S15. Bode phase angle plot of the DAAQ-COFs/GA electrode.

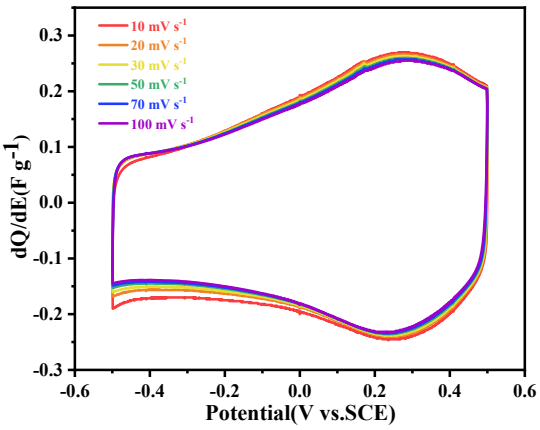

Figure S16. Differential capacity vs. potential curves for pure GA.

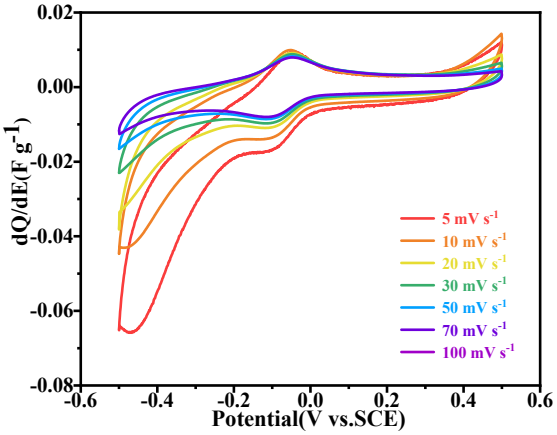

Figure S17. Differential capacity vs. potential curves for pure DAAQ-COFs.

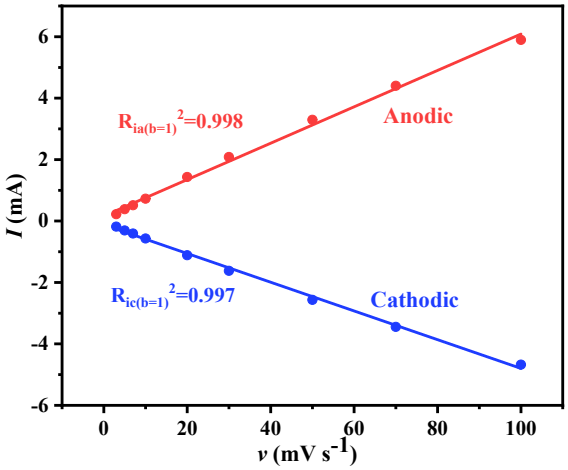

Figure S18. The relationship between peak specific current (*i*) and scan rate (*v*) of CV curves for DAAQ-COFs/GA at b = 1.

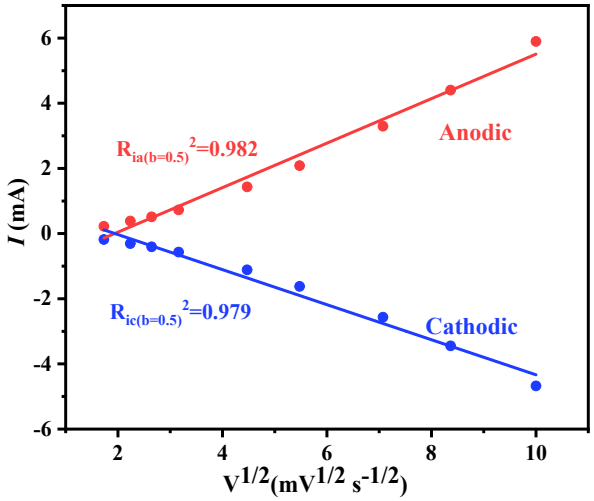

Figure S19. The relationship between peak specific current (*i*) and scan rate (*v*) of CV curves for DAAQ-COFs/GA at b = 0.5.

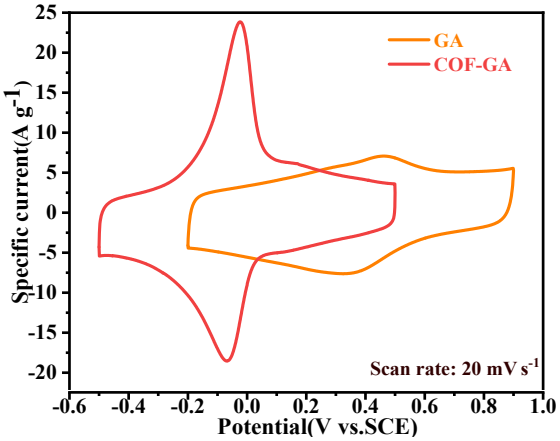

Figure S20. CV curves of the DAAQ-COFs and GA electrodes at a scan rate of 20 mV s^{-1} in a three-electrode system.

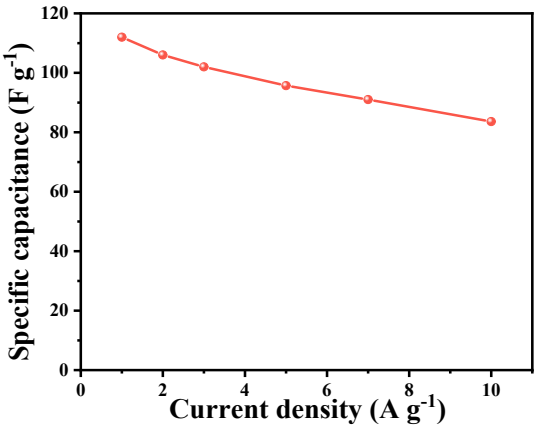

Figure S21. Specific capacitance of the ASC at various current densities.

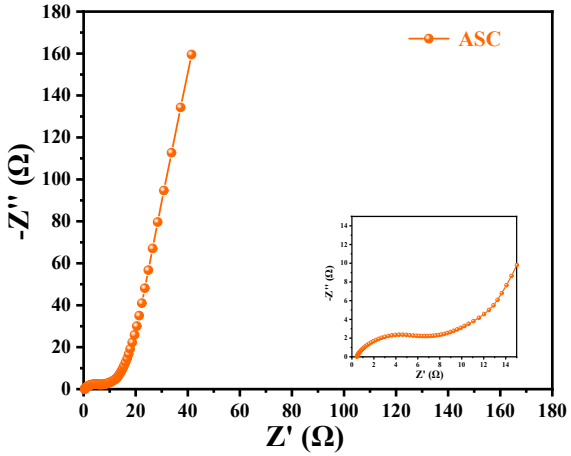

Figure S22. Nyquist plot of the ASC (the inset shows the high-frequency region).

Table S1 Performance comparison of related two-electrode systems.

Systems	Electrolyte	V_{cell} (V)	Energy density (Wh kg^{-1})	Power density (W kg^{-1})	Ref.
4KT-Tp COF//AC	1 M H_2SO_4	1.4	12.5	240	[3]
PDC−MA−COF//AC	6 M KOH	1.5	29.2	750	[4]
TaPa-Py//TaPa-Py	1 M H_2SO_4	0.8	9.06	100	[5]
TFP-NDA-COF	1 M H_2SO_4	1.2	28.4	2434	[6]
NH_2-f-MWCNT@$COF_{TTA-DHTA}$//AC	1 M Na_2SO_4	0.8	11.33	272	[7]
RuO2//Hex-Aza-COF-3	PVA-H2SO4 gel	1.7	23.3	661.2	[8]
rGO/COF-20//rGO/COF-20	1 M H_2SO_4	1.0	10.3	50	[9]
DAAQ-COFs/GA//GA	1 M H_2SO_4	1.4	30.5	701.2	**This work**

Supplementary References

1. N. I. Kovtyukhova, P. J. Ollivier, B. R. Martin, T. E. Mallouk, S. A. Chizhik, E. V. Buzaneva and A. D. Gorchinskiy, *Chemistry of Materials*, 1999, **11**, 771-778.
2. N. An, F. Zhang, Z. Hu, Z. Li, L. Li, Y. Yang, B. Guo and Z. Lei, *RSC Advances*, 2015, **5**, 23942-23951.
3. M. Li, J. Liu, Y. Li, G. Xing, X. Yu, C. Peng and L. Chen, *CCS Chemistry*, 2021, **3**, 696-706.
4. L. Li, F. Lu, R. Xue, B. Ma, Q. Li, N. Wu, H. Liu, W. Yao, H. Guo and W. Yang, *ACS Applied Materials & Interfaces*, 2019, **11**, 26355-26363.
5. A. M. Khattak, Z. A. Ghazi, B. Liang, N. A. Khan, A. Iqbal, L. Li and Z. Tang, *Journal of Materials Chemistry A*, 2016, **4**, 16312-16317.
6. S. K. Das, K. Bhunia, A. Mallick, A. Pradhan, D. Pradhan and A. Bhaumik, *Microporous and Mesoporous Materials*, 2018, **266**, 109-116.
7. B. Sun, J. Liu, A. Cao, W. Song and D. Wang, *Chem Commun (Camb)*, 2017, **53**, 6303-6306.
8. S. Kandambeth, J. Jia, H. Wu, V. S. Kale, P. T. Parvatkar, J. Czaban-Jóźwiak, S. Zhou, X. Xu, Z. O. Ameur, E. Abou-Hamad, A. H. Emwas, O. Shekhah, H. N. Alshareef and M. Eddaoudi, *Advanced Energy Materials*, 2020, **10**, 2001673.
9. C. Wang, F. Liu, J. Chen, Z. Yuan, C. Liu, X. Zhang, M. Xu, L. Wei and Y. Chen, *Energy Storage Materials*, 2020, **32**, 448-457.